Organic & Biomolecular Chemistry

ROYAL SOCIETY OF CHEMISTRY

PAPER

View Article Online
View Journal | View Issue

Cite this: *Org. Biomol. Chem.*, 2021, **19**, 2456

Synthesis and characterization of bichromophoric 1-deoxyceramides as FRET probes†

Eduardo Izquierdo,[a,b] Mireia Casasampere,[b] Gemma Fabriàs,[b,c] José Luís Abad,[b] Josefina Casas*[b,c] and Antonio Delgado*[a,b]

Received 21st January 2021,
Accepted 22nd February 2021

DOI: 10.1039/d1ob00113b

rsc.li/obc

The suitability as FRET probes of two bichromophoric 1-deoxydihydroceramides containing a labelled spisulosine derivative as a sphingoid base and two differently ω-labelled fluorescent palmitic acids has been evaluated. The ceramide synthase (CerS) catalyzed metabolic incorporation of ω-azido palmitic acid into the above labeled spisulosine to render the corresponding ω-azido 1-deoxyceramide has been studied in several cell lines. In addition, the strain-promoted click reaction between this ω-azido 1-deoxyceramide and suitable fluorophores has been optimized to render the target bichromophoric 1-deoxydihydroceramides. These results pave the way for the development of FRET-based assays as a new tool to study sphingolipid metabolism.

Introduction

Sphingolipids (SLs) are one of the major classes of lipids in eukaryotes. Canonical SLs derive from the sphingoid base dihydrosphingosine (dhSo) or (2*R*,3*S*) 2-amino-1,3-octadecanediol (Scheme 1), which is metabolically modified to account for the different families of SLs known to date.[1] Among them, ceramides (Cer) occupy a pivotal position in the metabolic pathways and they are considered as a metabolic hub.[2] Apart from their fundamental structural role in cell membranes,[3] Cer are also important second messengers in several cellular processes. In this regard, Cer have been reported to activate apoptosis in response to a variety of cell stress inducing agents[4–6] and, consistent with their role in apoptosis, various types of cancer cells have been shown to reduce their Cer levels as a survival strategy through the overexpression of CDase enzymes.[7] Furthermore, Cer also participate in the regulation of autophagy and stimulate cell cycle arrest, cell differentiation,[8] and senescence, the last by modifying telomerase activity.[9]

The intracellular levels of Cer are the result of the catabolic processes from higher SLs (sphingomyelin, glycosphingolipids and ceramide-1-phosphate), together with biosynthesis *de novo* by the *N*-acylation of dhSo with a variety of fatty acids (FA), prior to their desaturation by a specific desaturase (Des1) that introduces a C4(*E*) double bond into the sphingoid base. In this context, ceramide synthases (CerS) are a family of enzymes responsible for the *N*-acylation of dhSo (in the *de novo* pathway) or So (in the catabolic pathway) to form dhCer and Cer, respectively (Scheme 1).

Six isoforms of CerS have been identified in mammals, each one of them encoded by a unique gene (CerS1-6).[10] CerS enzymes are expressed differently in various tissues[11] and their levels of expression change during development, suggesting that populations of Cer with particular acyl chain lengths might be generated to meet the specific physiological needs of each tissue.[12] Moreover, the nature of the acyl chains is a determinant of the biophysical properties of the resulting Cer and also the signaling pathways in which they participate.[13] The development of modern lipidomic techniques[14] has allowed determination of the relative abundance of the various Cer types in a range of biological contexts, and has provided some insight into the effect of the acyl chain composition on the physiological role of Cer.[15] Given the importance of CerS activity in cell fate, we became interested in the development of new chemical probes[16] towards this end. In a previous work, we reported on the use of 1-deoxydihydrosphingosine (doxdhSo, spisulosine or ES285) as a suitable probe for the profiling of CerS activity in intact cells.[17] On the basis that 1-deoxysphingolipids (doxSLs) can be virtually considered as "dead-end" metabolites, due to the lack of the C1-OH group, we envisioned that a fluorescent probe derived from spisulosine, together with a suitable FA ana-

[a]*Department of Pharmacology, Toxicology and Medicinal Chemistry, Unit of Pharmaceutical Chemistry (Associated Unit to CSIC). Faculty of Pharmacy and Food Sciences. University of Barcelona (UB), Joan XXIII 27-31, 08028 Barcelona, Spain. E-mail: antonio.delgado@ub.edu*

[b]*Research Unit on BioActive Molecules, Department of Biological Chemistry, Institute for Advanced Chemistry of Catalonia (IQAC-CSIC), Jordi Girona 18-26, 08034-Barcelona, Spain. E-mail: fina.casas@iqac.csic.es*

[c]*Liver and Digestive Diseases Networking Biomedical Research Centre (CIBEREHD), ISCIII, 28029 Madrid, Spain*

†Electronic supplementary information (ESI) available: Calculated spectral overlap integrals and Förster critical distances (Table S1), photophysical properties of the monochromophoric compounds (Table S2), photophysical properties of the bichromophoric compounds (Table S3), and the NMR spectra of the synthesized compounds. See DOI: 10.1039/d1ob00113b

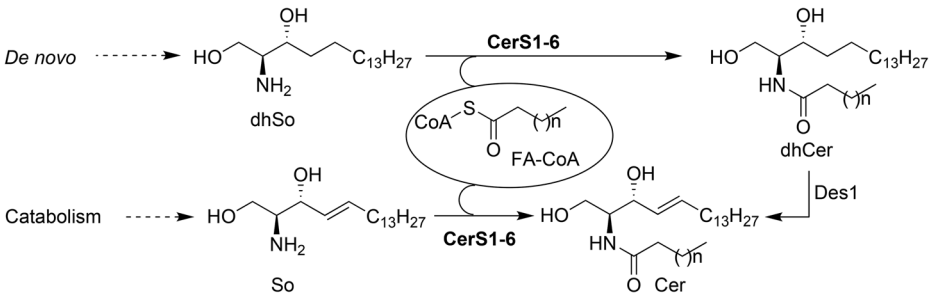

Scheme 1 Metabolic routes leading to Cer.

logue, could be used to develop a FRET-based assay to monitor CerS activity.[18]

The affinity towards lipid phases, fluorescent properties and sensitivity to the polarity of the surrounding environment of the fluorophores NBD and Nile red (NR) has promoted the use of these groups in several biological applications related to the study of the cell membrane.[19,20] Due to the existing overlap between the emission band of NBD and the absorption band of NR, these two fluorophores have also been incorporated into lipids as a donor–acceptor fluorophore pair to perform FRET experiments.[21–24] More recently, 7-methoxycoumarin-3-carboxylate (MCC) has also been used as an alternative fluorophore partner for NBD in FRET experiments.[25] In this case, however, NBD played the role of the acceptor fluorophore, whereas MCC was used as the donor. On this basis, we considered the NBD-labelled spisulosine **RBM5-155** and the ω-azido palmitic acid (ωN$_3$PA) as suitable CerS substrates for an ideal experiment design. A strained-promoted alkyne–azide cycloaddition (SPAAC) of the resulting doxdhCer **RBM5-159** with a BCN-derived fluorescent dye (**RBM5-142** (MCC) or **RBM5-143** (NR)) should render the bichromophoric doxdhCer **RBM5-160** or **RBM5-161**, respectively, whose FRET emission should correlate with CerS activity (Scheme 2).

In this paper, we wish to report on the synthesis and photochemical characterization of the above probes and reagents, their validation as CerS substrates and their suitability as FRET partners.[18]

Synthesis of the probes

The synthesis of the NBD probe **RBM5-155** was carried out as depicted in Scheme 3. Starting from the *anti*-configured allylic alcohol **RBM5-084**,[26] a cross-metathesis reaction with the bromoalkene **RBM5-149**, using the second generation Grubbs'

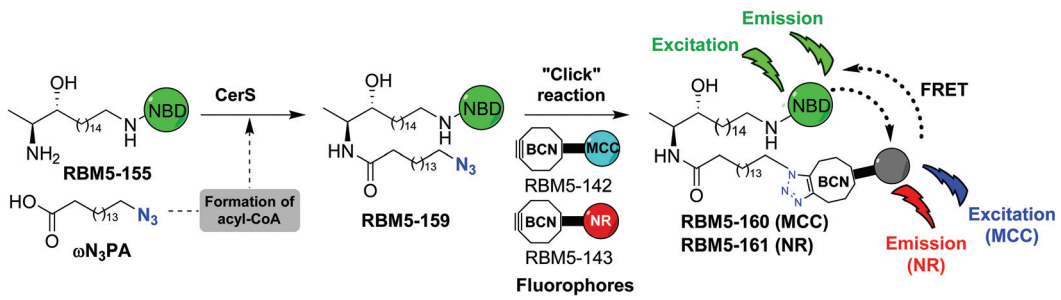

Scheme 2 Conceptual design of the required probes for a FRET-based CerS assay.

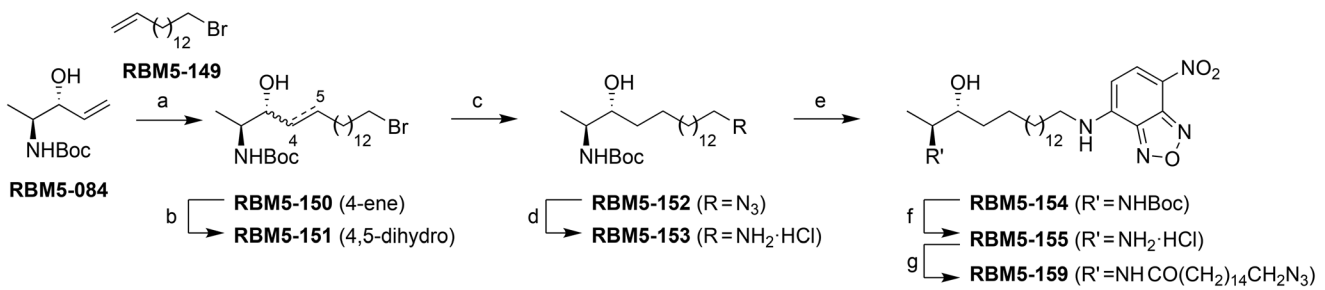

Scheme 3 Synthesis of doxSL probes. Reagents and conditions: (a) **RBM5-149**, Grubbs' 2nd gen. catalyst, CH_2Cl_2, reflux, 2 h, 44%, *E*/*Z* = 95 : 5; (b) H_2, 5 wt% Rh on Al_2O_3, MeOH, rt, 3 h, 86%; (c) NaN_3, DMF, 80 °C, 3 h, 95%; (d) TES, Pd–C, MeOH : $CHCl_3$ (9 : 1), rt, 10 min, 85%; (e) NBD-Cl, DIPEA, MeOH, 0 °C to rt, overnight, 84%; (f) AcCl, MeOH, 0 °C to rt, overnight, 80%; (g) ωN$_3$PA, EDC, HOBt, EtN_3, CH_2Cl_2, rt, 2 h, 74%.

catalyst, afforded a highly *E*-enriched *E* : *Z* mixture of **RBM5-150**, in agreement with the literature.[26] This mixture was subjected to catalytic hydrogenation on Rh/Al_2O_3 to give the corresponding saturated ω-bromo intermediate **RBM5-151**. Subsequent nucleophilic displacement with sodium azide, followed by the reduction of the azido group with the Pd/C-TES system,[27] reaction of the intermediate amine hydrochloride with NBD-Cl,[24] and final *N*-Boc removal afforded **RBM5-155**, which was isolated and further manipulated as the corresponding hydrochloride, given its apparent sensitivity to the alkaline conditions required for the formation of the free amine.[28] Finally, the *N*-acylation of **RBM5-155** with ωN_3PA[29] afforded the doxdhCer **RBM5-159**, which was used as the standard for quantitative LC-MS in cell assays (see below).

The fluorophores required for the SPAAC click reactions were obtained from the modified ω-aminoalkyl MCC and NR derivatives **RBM5-135** and **RBM5-136**, respectively, obtained as shown in Scheme 4.[18]

The clickable reagents **RBM5-142** and **RBM5-143** were synthesized by the condensation of **RBM5-135** and **RBM5-136**, respectively, with the *p*-nitrophenyl carbonate **RBM5-141**, obtained by the reaction of commercial *trans*-9-hydroxymethyl[6.1.0]bicyclonon-4-yne (BCN-OH) with 4-nitrophenyl chloroformate.[30] The corresponding bichromophoric click adducts **RBM5-160** and **RBM5-161** were prepared for their complete photochemical characterization and as standards for FRET studies (Scheme 5).

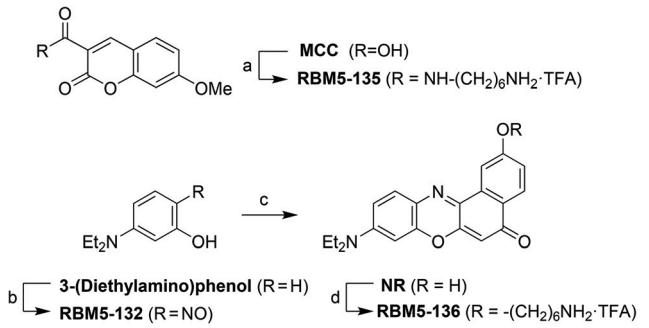

Scheme 4 Synthesis of the MCC and NR fluorophores. (a) (1). *N*-Boc-1,6-hexanediamine, EDC, HOBt, Et_3N, CH_2Cl_2, rt, 2 h, 57%; (2). TFA : CH_2Cl_2 (1 : 2), 0 °C to rt, 1 h, quantitative; (b) $NaNO_2$, HCl (aq.), 0 °C, 5 h, 67%; (c) naphthalene-1,6-diol, DMF, 160 °C, 4 h, 19%; (d) (1). *N*-Boc-6-bromohexanamine, K_2CO_3, DMF, 85 °C, overnight, 78%; (2). TFA : CH_2Cl_2 (1 : 2), 0 °C to rt, 1 h, quantitative.

FRET efficiency of the bichromophoric probes RBM5-160 and RBM5-161

The suitability of the selected FRET partners was corroborated by calculation of the spectral overlap integral and Förster radius (R_0) (Table S1†) from the spectral data of the monochromophoric compounds **RBM5-142**, **RBM5-143** and **RBM5-154** (Table S2†). The normalized absorption and emission spectra of the bichromophoric probes **RBM5-160** and **RBM5-161** in DMSO, EtOH and PBS buffer presented two bands owing to the presence of the two fluorescent labels (Fig. 1). Compound **RBM5-160** presented two maxima at around 350 nm (MCC moiety) and 470 nm (NBD moiety), while the maxima for **RBM5-161** were located around 485 nm (NBD moiety) and 550 nm (NR moiety). The fluorescence intensity was strongly affected by the solvent, the highest fluorescence intensities being recorded in EtOH for both compounds. However, their emission in PBS buffer was reduced as a result of their lower aqueous solubility. The position and shape of the emission spectra in the two probes were slightly modified in the different solvents, due to the solvatochromic effects. Furthermore, there were also considerable deviations in the absorption spectra of compounds **RBM5-160** and **RBM5-161**, when compared with the spectra of the related monochromophoric compounds, probably due to the intramolecular attractive interactions between the two fluorophores in each compound.[31] The molar extinction coefficients (ε) of compounds **RBM5-160** and **RBM5-161**, calculated at their corresponding two absorption maxima in DMSO and EtOH are listed in Table S3.†

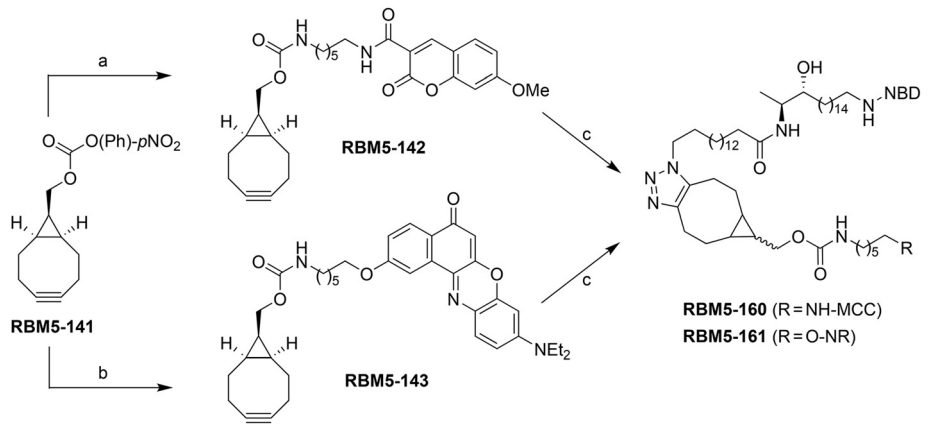

Scheme 5 Synthesis of clickable fluorophores. Reagents and conditions: (a) **RBM5-135**, Et_3N, CH_2Cl_2, rt, overnight, 89%; (b) **RBM5-136**, Et_3N, CH_2Cl_2, rt, overnight (90%); (c) **RBM5-159**, CH_2Cl_2, rt, overnight, 84–93% (for assay-like conditions, see text).

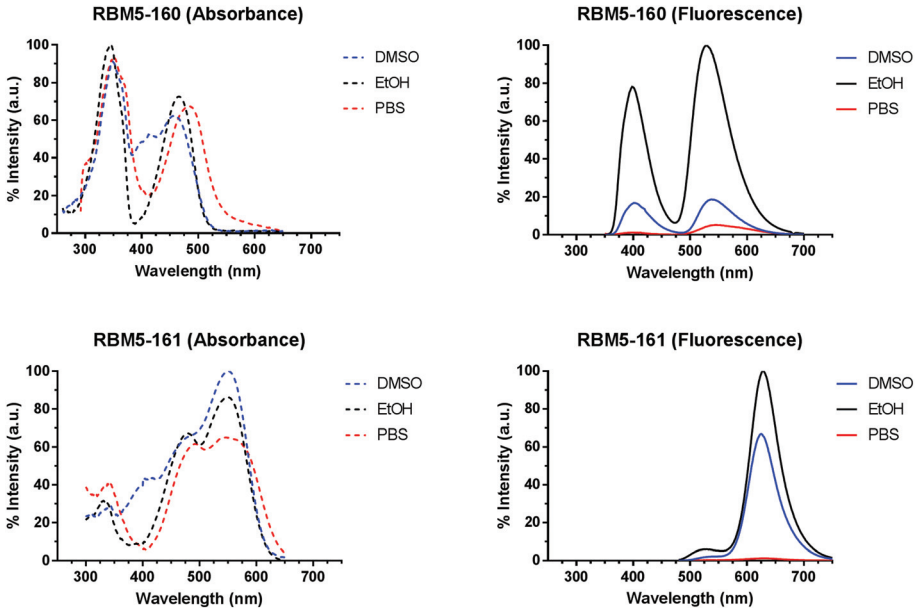

Fig. 1 Normalised absorption (left panels) and emission (right panels) spectra for the bichromophoric compounds **RBM5-160** (top) and **RBM5-161** (bottom) at 5 μM in DMSO (blue), EtOH (black) and PBS (red). Emission spectra upon excitation at 340 nm (MCC in **RBM5-160**) and 455 nm (NBD in **RBM5-161**), respectively. The absorption and emission spectra of **RBM5-160** in DMSO and PBS were normalised to those of the same compound in EtOH. The absorption spectra of **RBM5-161** in EtOH and PBS were normalised to those in DMSO. The emission spectra of **RBM5-161** in DMSO and PBS were normalised to those in EtOH.

The intramolecular FRET efficiencies of compounds **RBM5-160** and **RBM5-161** were estimated in DMSO and EtOH, based on the loss of donor fluorescence in the presence of the acceptor. To this end, we compared the integrated fluorescence intensities (I), within the donor-specific wavelength interval, of the donor (D) compounds (**RBM5-142** and **RBM5-154**) to those of the related donor + acceptor (DA) compounds (**RBM5-160** and **RBM5-161**, respectively). The calculated FRET efficiency of the NBD/NR pair in **RBM5-161** ($E_{NBD/NR}$ = 0.88–0.96) was higher than that of the MCC/NBD pair in **RBM5-160** ($E_{MCC/NBD}$ = 0.56–0.88). For both fluorophore pairs, the FRET process was more efficient in EtOH than in DMSO and, in the case of the NBD/NR pair in **RBM5-161**, the two studied excitation wavelengths gave the same E value in EtOH (Table 1).

Table 1 Study of the intramolecular FRET efficiency of the bichromophoric compounds **RBM5-160** and **RBM5-161**

Compound	Solvent	λ_{ex} (nm)	E^a
RBM5-160	DMSO	340	0.56
	EtOH	340	0.86
RBM5-161	DMSO	470	0.90
		455	0.88
	EtOH	470	0.96
		455	0.96

[a] FRET efficiencies (E) were calculated from the decrease of the donor emission (see Experimental section).

Optimization of the SPAAC reaction from RBM5-159

The SPAAC reaction between the azide-tagged doxdhCer **RBM5-159** and the fluorescent dyes **RBM5-142** and **RBM5-143** was studied under different conditions in order to determine the best reagent ratios and reaction times at a concentration scale compatible with that expected in the CerS activity assay in intact cells. The reaction progress was first monitored in DMSO by analyzing the changes in the fluorescence emission of the mixture upon irradiation at the donor-specific excitation wavelength. For **RBM5-160** (donor: MCC, acceptor: NBD, see Scheme 2), the fluorescence emission at λ_{em} = 535 (NBD emission) at two single concentrations of **RBM5-159** (5 and 20 μM) and increasing concentrations of the BCN-MCC reagent **RBM5-142** (from 5 to 50 μM) was always lower than that of a standard solution of the expected adduct **RBM5-160** at 5 and 20 μM (results not shown). However, a similar experiment using the BCN-NR reagent **RBM5-143** (from 5 to 50 μM) led to fluorescence intensities at λ_{em} = 625 (NR emission) comparable to those of a standard solution of the expected adduct **RBM5-161** using a 2.5 to 4 fold excess of the BCN-NR reagent **RBM5-143** (Fig. 2).

Experiments in MeOH, EtOH and sodium acetate buffer (NaOAc 250 mM, NaCl 200 mM, 0.1% Triton X-100) also showed a remarkable enhancement of the emission at 625 nm (acceptor emission, λ_{exc} = 455 nm) in comparison with **RBM5-159**, together with an attenuation of the fluorescence emission

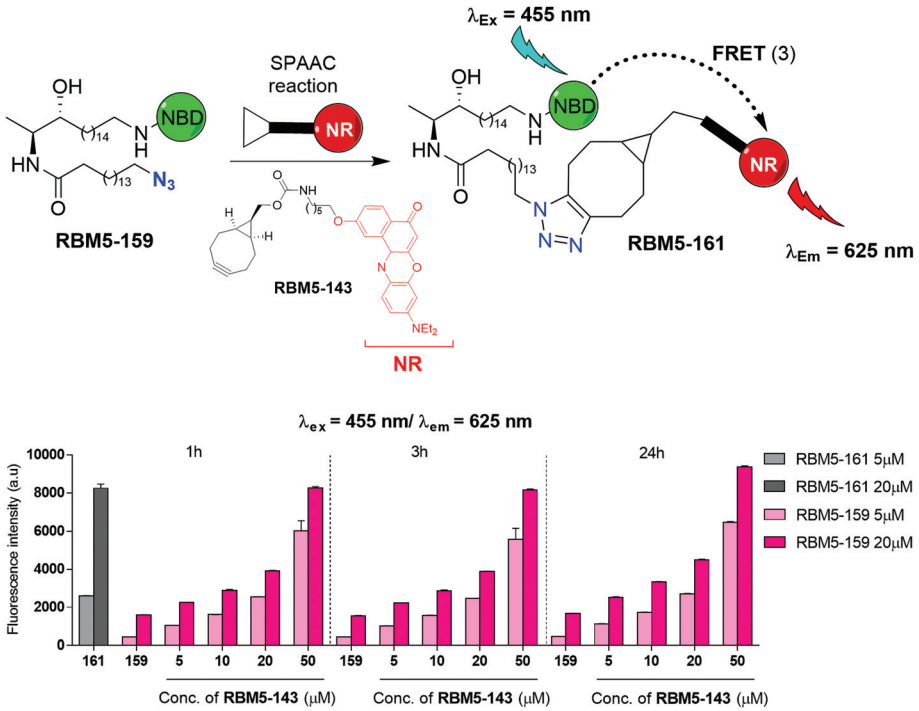

Fig. 2 Bar diagram representing the changes in fluorescence emission at 625 nm (bottom), resulting from the excitation at 455 nm, of mixtures containing different ratios of compounds **RBM5-159** and **RBM5-143** in DMSO at various reaction times. Compound **RBM5-159** was used as the negative control, equivalent to 0% conversion, whereas compound **RBM5-161** was used as the positive control, equivalent to 100% conversion. The results correspond to the mean ± standard deviation of at least two independent experiments with triplicates.

at 535 nm (donor emission, λ_{exc} = 455 nm), in agreement with the formation of the desired cycloadduct **RBM5-161** (Fig. S1†). The background emission of **RBM5-143** at 625 nm observed at the donor excitation (λ_{exc} = 455 nm) is indicative of an excitation cross-talk (or acceptor excitation bleed-through, AEB), a phenomenon related to the overlap of the donor and acceptor absorption spectra. This phenomenon, together with the related emission cross-talk (or donor emission bleed-through, DEB), arising from the overlap of the donor and acceptor emission spectra[32] must be carefully considered in the design of ratiometric experiments based on the development of the FRET effect. In contrast, ratiometric experiments based on FRET attenuation[21,22,24] may benefit from the disappearance of these interferences. The experimental AEB and DEB calculated for **RBM5-161** are listed in Table S4 and Fig. S2, S3.†

CerS catalyzed incorporation of ω-azidopalmitic acid into RBM5-155 in cells

The suitability of the probe **RBM5-155** and ωN_3PA as CerS substrates was evaluated by examining the extent of their metabolic conversion into the corresponding *N*-acylated doxdhCer **RBM5-159** by LC-MS. Initial experiments were carried out in lung adenocarcinoma A549 cells and mouse embryonic fibroblasts (MEF). Even though the total amount of doxdhCers, arising from acylation of **RBM5-155** with endogenous FAs, was very similar in the two cell lines (~120–130 pmol equiv./10^6 cells), the profile of the different doxdhCer species differed considerably. In A549 cells, there was a high proportion of elongated $C18N_3$ and $C20N_3$ doxdhCer species (resulting from the action of the endogenous elongases),[33] whereas the non-elongated doxdhCer **RBM5-159** accounted for less than a third of the total doxdhCers (~28%). Conversely, in MEF cells, the non-elongated **RBM5-159** was the most abundant metabolite (85% of the total doxdhCers), whereas the formation of elongated species was minimal. These results show that the elongation process is unpredictable and highly dependent on the cell line, although it appears to be independent on the overall CerS activity. Attempts to reduce or avoid the acyl chain elongation by using the FA biosynthesis inhibitors TOFA or cerulenin were fruitless.[34–36] Moreover, the incorporation of ωN_3C13 acid, as well as that of branched αN_3PA and $(\omega\text{-}1)N_3$PA, was also tested. The first two were deemed as poor CerS substrates since only modest amounts of the corresponding doxdhCers were formed under the standard assay. Conversely, the branched $(\omega\text{-}1)N_3$PA was efficiently incorporated, although the high ratio of the elongated doxdhCer observed made us disregard its use (results not shown). For practical purposes, the overexpression of the CerS under study may improve the signal-to-noise ratio of the assay. As a proof of concept, human embryonic kidney cells (HEK293T) were transfected with the

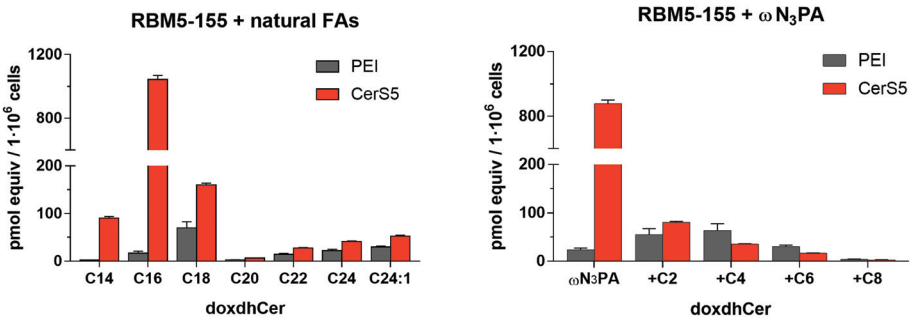

Fig. 3 *N*-Acylation of the doxdhSo probe **RBM5-155** with the endogenous natural FAs or ωN_3PA. HEK293T cells transfected with the plasmid containing human CerS5 (bars in orange) or simply treated with the transfection reagent PEI (bars in grey) were incubated for 90 min with **RBM5-155** (5 μM) in the absence (left) or in the presence (right) of ωN_3PA (0.5 mM) complexed in 0.5% acid-free BSA. After lipid extraction, the different doxdhCer species were quantified by UPLC–TOF. Left: Amount of doxdhCers containing endogenous natural FAs; right: amount of doxdhCers containing the administered ωN_3PA and the corresponding elongated FAs. The results correspond to the mean ± standard deviation of at least two independent experiments with triplicates.

human CerS5 gene using the cationic polymer polyethylenimine (PEI),[37] and were subsequently incubated with the doxdhSo probe **RBM5-155** and ωN_3PA. UPLC-TOF analysis of the lipid extracts showed a higher ratio of the C16-doxdhCer species in the transfected cells, in agreement with the expected preference of the CerS5 isoform for the C16 FAs[38] (Fig. 3).

Conclusions

In summary, the NBD probe **RBM5-155** and the modified fatty acid ωN_3PA behave as suitable CerS substrates in cells. Despite the degree of incorporation and elongation of the fatty acid being strongly dependent on the particular cell line, studies carried out with the doxdhCer **RBM5-159** indicated its suitability as a SPAAC reaction partner with the BCN modified NR fluorophore **RBM5-143** to render the bichromophoric doxdhCer **RBM5-161**, exhibiting a high FRET efficiency in the solvent systems used. These results represent an interesting addition to the available chemical toolbox of labelled sphingolipids for FRET-based studies in cells. Efforts along this line are underway in our lab and will be reported in due course.

Experimental section

Synthesis

General procedures. All chemicals were purchased from commercial sources and used as received unless otherwise noted. Dry solvents (THF, DMF and CH_2Cl_2), obtained from a PureSolv dispenser and subsequently degassed with an inert gas, were used in most reactions. Synthesis grade (hexane, EtOAc, Et_2O and CH_2Cl_2) or HPLC-grade (MeOH) solvents were used for extractions and purifications. Progression of the reactions was controlled by thin layer chromatography (TLC), using ALUGRAM® SIL G/UV254 (Macherey-Nagel) silica gel precoated aluminum sheets (layer: 0.2 mm, silica gel 60). Compounds were detected by using UV light (λ = 254 nm) and a stain solution of phosphomolibdic acid (5.7% in EtOH). Usual work up refers to washing of the combined organic layers with brine (2 × 25 mL), drying over anhydrous $MgSO_4$ and concentration to dryness. Compounds were purified by flash column chromatography, using silica gel (Chromatogel 60 Å, 35–75 μm) as the stationary phase. Mobile phases and gradients are specified in each case. ^{1}H and ^{13}C nuclear magnetic resonance spectra were recorded on a Varian – Mercury 400 (^{1}H NMR at 400 MHz and ^{13}C NMR at 100.6 MHz) spectrometer using $CDCl_3$ or CD_3OD as solvent. Chemical shifts of deuterated solvents were used as internal standards. Chemical shifts are given in parts per million (ppm) and coupling constants (J) in hertz (Hz). Splitting patterns have been described as a singlet (s), broad singlet (br s), doublet (d), triplet (t), quartet (q), quintuplet (p), multiplet (m), apparent (app) or combinations of these descriptive names. Specific optical rotations were recorded on a digital PerkinElmer 34 polarimeter at 25 °C in a 1 dm, 1 mL cell, using a sodium light lamp (λ = 589 nm). Specific optical rotation values ($[\alpha]_D$) are expressed in deg^{-1} cm^3 g^{-1}, and concentrations (c) are reported in g per 100 mL of solvent. High-resolution mass spectra (HRMS) were recorded Waters Aquity UPLC system connected to a Waters LCT Premier Orthogonal Accelerated Time of Flight Mass Spectrometer (Waters, Milford, MA, USA) operated in the positive electrospray ionisation mode. Samples were analyzed by FIA (Flow Injection Analysis), using ACN/water (70 : 30) as the mobile phase. Samples were analyzed using a 10 μL volume injection. The m/z ratios are reported as values in atomic mass units.

((1R,8S,9S)-Bicyclo[6.1.0]non-4-yn-9-yl)methyl (6-(7-methoxy-2-oxo-2H-chromene-3-carboxamido)hexyl)carbamate ***(RBM5-142).*** To an ice-cooled solution of *N*-Boc protected **RBM5-135** [18] (93 mg, 0.22 mmol) in dry CH_2Cl_2 (6 mL) was added dropwise neat TFA (1.5 mL). After stirring at rt for 2 h in the dark, the reaction mixture was concentrated to dryness to afford the corresponding crude amine trifluoroacetate (71 mg). This crude was taken up in CH_2Cl_2 (10 mL), followed by the sequential addition of Et_3N (108 μL, 0.78 mmol) and *p*-nitrophenol

activated carbonate ester **RBM5-141** [30] (70 mg, 0.22 mmol). After stirring overnight at rt in the dark, the reaction mixture was evaporated *in vacuo* and the residue was flash chromatographed (from 0 to 20% EtOAc in CH_2Cl_2) to give the desired carbamate **RBM5-142** (98 mg, 89%) as an off-white solid.

^{1}H NMR (400 MHz, $CDCl_3$) δ 8.83 (s, 1H), 8.76 (br s, 1H), 7.58 (d, J = 8.7 Hz, 1H), 6.93 (dd, J = 8.7, 2.4 Hz, 1H), 6.86 (d, J = 2.4 Hz, 1H), 4.69 (br s, 1H), 4.13 (d, J = 8.1 Hz, 2H), 3.91 (s, 3H), 3.44 (td, J = 7.1, 5.8 Hz, 2H), 3.20–3.12 (m, 2H), 2.34–2.15 (m, 6H), 1.67–1.24 (m, 11H), 0.99–0.86 (m, 2H).

^{13}C NMR (101 MHz, $CDCl_3$) δ 164.9, 162.1, 162.1, 156.9, 156.8, 148.3, 131.0, 115.0, 114.1, 112.6, 100.4, 99.0, 62.7, 56.2, 41.0, 39.7, 30.0, 29.5, 29.2, 26.7, 26.5, 21.6, 20.2, 18.0.

HRMS calcd for $C_{28}H_{35}N_2O_6$ ($[M + H]^+$): 495.2490, found: 495.2496.

*((1R,8S,9S)-Bicyclo[6.1.0]non-4-yn-9-yl)methyl (6-((9-(diethylamino)-5-oxo-5H-benzo[a]phenoxazin-2-yl)oxy)hexyl)carbamate (**RBM5-143**).* To an ice-cooled solution of *N*-Boc protected **RBM5-136** [18] (100 mg, 0.19 mmol) in dry CH_2Cl_2 (6 mL) was added dropwise neat TFA (1.5 mL). After stirring at rt for 2 h in the dark, the reaction mixture was concentrated to dryness to afford the corresponding crude amine trifluoroacetate (81 mg). This crude was taken up in CH_2Cl_2 (10 mL), followed by the sequential addition of Et_3N (93 μL, 0.67 mmol) and *p*-nitrophenol activated carbonate ester **RBM5-141** [30] (60 mg, 0.19 mmol). After stirring overnight at rt in the dark, the reaction mixture was evaporated *in vacuo* and the residue was flash chromatographed (from 0 to 20% EtOAc in CH_2Cl_2) to give the desired carbamate **RBM5-143** (104 mg, 90%) as a shiny dark-red solid.

^{1}H NMR (400 MHz, $CDCl_3$) δ 8.21 (d, J = 8.7 Hz, 1H), 8.03 (d, J = 2.6 Hz, 1H), 7.60 (d, J = 9.0 Hz, 1H), 7.15 (dd, J = 8.7, 2.6 Hz, 1H), 6.65 (dd, J = 9.1, 2.7 Hz, 1H), 6.45 (d, J = 2.7 Hz, 1H), 6.29 (s, 1H), 4.70 (br s, 1H), 4.19–4.11 (m, 4H), 3.46 (q, J = 7.1 Hz, 5H), 3.25–3.15 (m, 2H), 2.34–2.16 (m, 6H), 1.90–1.82 (m, 2H), 1.67–1.30 (m, 10H), 1.26 (t, J = 7.0 Hz, 6H), 0.97–0.87 (m, 2H).

^{13}C NMR (101 MHz, $CDCl_3$) δ 183.4, 161.9, 156.9, 152.2, 150.9, 147.0, 140.3, 134.2, 131.2, 127.9, 125.7, 124.8, 118.4, 109.6, 106.7, 105.5, 99.0, 96.5, 68.3, 62.8, 45.2, 41.1, 30.1, 29.3, 29.2, 26.6, 25.9, 21.6, 20.2, 17.9, 12.8.

HRMS calcd for $C_{37}H_{44}N_3O_5$ ($[M + H]^+$): 610.3275, found: 610.3279.

*15-Bromopentadec-1-ene (**RBM5-149**).* A stirred solution of 14-pentadecen-1-ol [39] (2.77 g, 12.23 mmol) and PPh_3 (3.53 g, 13.46 mmol) in anhydrous CH_2Cl_2 (100 mL) was cooled to 0 °C, and NBS (2.61 g, 14.68 mmol) was added in small portions over 10 min. The resultant dark yellow solution was allowed to warm to rt and stirred for 1 h, after which the solvent was removed by vacuum evaporation. The residue was then diluted with water (50 mL), extracted with hexanes (3 × 50 mL) and worked-up as usual to give a crude, which was purified by flash chromatography on silica gel (isocratic 100% hexanes) to afford **RBM5-149** as a colorless oil, (2.62 g, 74%).

^{1}H NMR (400 MHz, $CDCl_3$) δ 5.81 (ddt, J = 16.9, 10.2, 6.7 Hz, 1H), 4.99 (dq, J = 17.1, 1.9 Hz, 1H), 4.93 (ddt, J = 10.2, 2.4, 1.4 Hz, 1H), 3.41 (t, J = 6.9 Hz, 2H), 2.08–2.00 (m, 2H), 1.85 (dt, J = 14.5, 7.0 Hz, 2H), 1.46–1.33 (m, 3H), 1.32–1.25 (m, 16H).

^{13}C NMR (101 MHz, $CDCl_3$) δ 139.4, 114.2, 34.2, 34.0, 33.0, 29.8, 29.8, 29.7, 29.7, 29.6, 29.3, 29.1, 28.9, 28.3.

*(2'S,3'R,4'EZ)-tert-Butyl (18-bromo-3-hydroxyoctadec-4-en-2-yl) carbamate (**RBM5-150**).* To a stirred solution of **RBM5-084** [26,40] (480 mg, 2.38 mmol) and olefin **RBM5-149** (1.59 g, 5.49 mmol) in degassed CH_2Cl_2 (20 mL), second generation Grubbs' catalyst (101 mg, 0.12 mmol) was added in one portion at rt. The resulting mixture was refluxed in the dark for 2 h, cooled to rt and concentrated *in vacuo* to afford a crude, which was purified by flash chromatography on silica gel (from 0 to 5% MTBE in CH_2Cl_2). Compound **RBM5-150** was obtained as an inseparable mixture of *E*/*Z* isomers (colourless thick oil, 485 mg, 44%).

^{1}H NMR (400 MHz, $CDCl_3$) (*E* isomer) δ 5.71 (dt, J = 14.6, 6.7 Hz, 1H), 5.42 (dt, J = 15.0, 7.5 Hz, 1H), 4.76 (br s, 1H), 4.11 (dd, J = 6.4, 3.0 Hz, 1H), 3.73–3.58 (m, 1H), 3.40 (t, J = 6.9 Hz, 2H), 2.09–1.96 (m, 2H), 1.85 (dt, J = 14.5, 6.9 Hz, 2H), 1.44 (s, 9H), 1.43–1.23 (m, 20H), 1.07 (d, J = 6.9 Hz, 3H).

^{13}C NMR (101 MHz, $CDCl_3$) (mixture of *E*/*Z* isomers) δ 156.1, 155.7, 134.2, 133.5, 129.4, 128.7, 125.6, 124.9, 79.4, 79.2, 75.4, 73.5, 51.0, 50.0, 37.3, 33.9, 33.4, 32.8, 32.6, 32.3, 29.6, 29.5, 29.5, 29.4, 29.2, 28.7, 28.4, 28.1, 15.2, 14.3.

*(2'S,3'R)-tert-Butyl (18-bromo-3-hydroxyoctadecan-2-yl)carbamate (**RBM5-151**).* A solution of **RBM5-150** (450 mg, 0.97 mmol) in degassed MeOH (45 mL) was hydrogenated at 1 atm and rt in the presence of Rh/Al_2O_3 (60 mg, 15% w/w). After stirring for 3 h, the catalyst was removed by filtration through a Celite® pad, and the solid was rinsed with MeOH (3 × 10 mL). The combined filtrates were concentrated *in vacuo*, and the residue was subjected to flash chromatography on silica gel (from 0 to 1% MeOH in CH_2Cl_2) to yield **RBM5-151** as a white solid (395 mg, 87%).

$[\alpha]_D^{20}$ = −3.65 (*c* 1, $CHCl_3$).

^{1}H NMR (400 MHz, $CDCl_3$) δ 4.74 (br s, 1H), 3.70–3.67 (m, 1H), 3.64 (td, J = 8.0, 7.2, 2.7 Hz, 1H), 3.41 (t, J = 6.9 Hz, 2H), 1.85 (dt, J = 14.5, 7.0 Hz, 2H), 1.71 (br s, 1H), 1.44 (s, 9H), 1.43–1.35 (m, 4H), 1.34–1.23 (m, 22H), 1.08 (d, J = 6.8 Hz, 3H).

^{13}C NMR (101 MHz, $CDCl_3$) δ 156.0, 79.6, 74.6, 50.8, 34.2, 33.6, 33.0, 29.8, 29.7, 29.6, 28.9, 28.6, 28.3, 26.2, 14.5.

HRMS calcd for $C_{23}H_{47}BrNO_3$ ($[M + H]^+$): 464.2734, 466.2713, found: 464.2729, 466.2718.

*(2'S,3'R)-tert-Butyl (18-azido-3-hydroxyoctadecan-2-yl)carbamate (**RBM5-152**).* To a stirred solution of **RBM5-151** (395 mg, 0.85 mmol) in anhydrous DMF (8 mL) was added NaN_3 (166 mg, 2.55 mmol). The mixture was heated to 80 °C and stirred for 3 h under Ar. Water (20 mL) was next added, and the mixture was extracted with Et_2O (3 × 20 mL). Usual workup afforded a crude, which was purified by flash chromatography (from 0 to 1% MeOH in CH_2Cl_2) to give **RBM5-152** (off-white wax, 346 mg, 95%).

$[\alpha]_D^{20}$ = −4.13 (*c* 1, $CHCl_3$).

^{1}H NMR (400 MHz, $CDCl_3$) δ 4.75 (s, 1H), 3.71–3.67 (m, 1H), 3.66–3.61 (m, 1H), 3.25 (t, J = 7.0 Hz, 2H), 1.75 (br s, 1H),

1.66–1.54 (m, 2H), 1.44 (s, 9H), 1.40–1.35 (m, 4H), 1.34–1.23 (m, 22H), 1.07 (d, J = 6.8 Hz, 3H).

^{13}C NMR (101 MHz, $CDCl_3$) δ 156.0, 79.6, 74.6, 51.6, 50.7, 33.6, 29.8, 29.8, 29.7, 29.7, 29.7, 29.7, 29.6, 29.3, 29.0, 28.5, 26.8, 26.2, 14.4.

HRMS calcd for $C_{23}H_{47}N_4O_3$ ($[M + H]^+$): 427.3643, found: 427.3636.

*(2'S,3'R)-tert-Butyl (18-amino-3-hydroxyoctadecan-2-yl)carbamate (**RBM5-153**).* To a solution of **RBM5-152** (300 mg, 0.70 mmol) in degassed MeOH (16 mL) containing Pd–C (60 mg, 20% w/w) neat TES (1.1 mL, 7.03 mmol) was added dropwise, and the resultant suspension was stirred at rt under an Ar-filled balloon. After stirring for 1 h, the reaction mixture was filtered through a pad of Celite® and the solid was rinsed with MeOH (3 × 5 mL). The combined filtrates were concentrated *in vacuo* and the residue was triturated with hexanes (4 × 2 mL) to give the desired amine hydrochloride, without the need of further purification.

^{1}H NMR (400 MHz, CD_3OD) δ 3.53–3.47 (m, 1H), 3.47–3.41 (m, 1H), 2.67 (t, J = 7.1 Hz, 2H), 1.53–1.46 (m, 4H), 1.44 (s, 9H), 1.30 (s, 24H), 1.08 (d, J = 6.6 Hz, 3H).

^{13}C NMR (101 MHz, CD_3OD) δ 157.8, 79.9, 75.3, 51.8, 42.3, 34.8, 33.0, 30.8, 30.7, 30.6, 28.8, 28.0, 27.1, 15.5.

HRMS calcd for $C_{23}H_{49}N_2O_3$ ($[M + H]^+$): 401.3738, found: 401.3742.

*(2'S,3'R)-tert-Butyl [3-hydroxy-18-[(7-nitrobenzo[c][1,2,5]oxadiazol-4-yl)amino]octadecan-2-yl]carbamate (**RBM5-154**).* To a stirred solution of 4-chloro-7-nitrobenzo[*c*][1,2,5]oxadiazole (NBD-Cl) (132 mg, 0.66 mmol) in MeOH (15 mL) containing DIPEA (522 μL, 3.00 mmol) at 0 °C was added dropwise a solution of **RBM5-153** (240 mg, 0.60 mmol) in MeOH (10 mL). After the addition was complete, the mixture was allowed to warm to rt and stirred overnight. Then, the volatiles were removed under reduced pressure and the residue was directly subjected to flash chromatography on silica gel (from 0 to 1% MeOH in CH_2Cl_2) to afford **RBM5-154** as a shiny orange wax (278 mg, 82%).

^{1}H NMR (400 MHz, $CDCl_3$) δ 8.49 (d, J = 8.6 Hz, 1H), 6.31 (br s, 1H), 6.17 (d, J = 8.7 Hz, 1H), 4.75 (br s, 1H), 3.73–3.66 (m, 1H), 3.66–3.62 (m, 1H), 3.49 (ap q, J = 6.7 Hz, 2H), 1.86 (br s, 1H), 1.81 (dt, J = 14.9, 7.4 Hz, 2H), 1.53–1.44 (m, 2H), 1.44 (s, 9H), 1.41–1.35 (m, 4H), 1.33–1.23 (m, 20H), 1.07 (d, J = 6.8 Hz, 3H).

^{13}C NMR (101 MHz, $CDCl_3$) δ 156.0, 144.3, 144.2, 144.0, 136.7, 123.7, 98.6, 79.6, 74.6, 50.8, 44.2, 33.6, 29.8, 29.7, 29.7, 29.7, 29.6, 29.6, 29.5, 29.3, 28.6, 28.5, 27.0, 26.1, 14.5.

HRMS calcd for $C_{29}H_{50}N_5O_6$ ($[M + H]^+$): 564.3756, found: 564.3761.

*(2S,3R)-2-Amino-18-[(7-nitrobenzo[c][1,2,5]oxadiazol-4-yl)amino]octadecan-3-ol hydrochloride (**RBM5-155**).* An ice-cooled solution of **RBM5-154** (85 mg, 0.15 mmol) in MeOH (10 mL) was treated with neat AcCl (54 μL, 0.75 mmol) and the resulting mixture was allowed to warm to rt and stirred overnight in the dark. Then, the solvent was evaporated *in vacuo* and the residue was purified by flash chromatography on silica gel (from 0 to 20% MeOH in CH_2Cl_2) to afford **RBM5-155** as a shiny orange wax (65 mg, 86%).

^{1}H NMR (400 MHz, CD_3OD) δ 8.52 (d, J = 8.7 Hz, 1H), 6.35 (d, J = 8.9 Hz, 1H), 3.75–3.65 (m, 1H), 3.53 (br s, 2H), 3.31–3.22 (m, 1H), 1.77 (app p, J = 7.4 Hz, 2H), 1.55–1.37 (m, 8H), 1.36–1.25 (m, 18H), 1.22 (d, J = 6.8 Hz, 3H).

^{13}C NMR (101 MHz, CD_3OD) δ 146.7, 145.8, 145.5, 138.6, 122.7, 99.6, 71.7, 52.6, 44.8, 34.0, 30.7, 30.6, 30.3, 29.2, 28.0, 27.0, 12.1.

HRMS calcd for $C_{24}H_{42}N_5O_4$ ($[M + H]^+$): 464.3231, found: 464.3228.

*(2'S,3'R)-16-Azido-N-[3-hydroxy-18-[(7-nitrobenzo[c][1,2,5]oxadiazol-4-yl)amino]octadecan-2-yl]hexadecanamide (**RBM5-159**).* EDC·HCl (12 mg, 64 μmol) and HOBt (7 mg, 52 μmol) were sequentially added to an ice-cooled solution of ω-azidopalmitic acid[29] (13 mg, 44 μmol) in anhydrous CH_2Cl_2 (6 mL). The resulting mixture was vigorously stirred at rt under Ar for 15 min, and next added dropwise to a solution of **RBM5-155** (20 mg, 40 μmol) and Et_3N (89 μL, 0.20 mmol) in anhydrous CH_2Cl_2 (6 mL), and the reaction was stirred at rt for additional 2 h. The mixture was next diluted with CH_2Cl_2 (50 mL), washed with brine (2 × 25 mL) and worked-up as usual to afford a crude, which was flash chromatographed (from 0 to 14% EtOAc in CH_2Cl_2) to afford **RBM5-159** as a shiny orange solid (22 mg, 74%).

^{1}H NMR (400 MHz, $CDCl_3$) δ 8.48 (d, J = 8.6 Hz, 1H), 6.49 (br s, 1H), 6.17 (d, J = 8.7 Hz, 1H), 5.81 (d, J = 7.9 Hz, 1H), 4.05–3.96 (m, 1H), 3.66–3.59 (m, 1H), 3.53–3.45 (m, 2H), 3.24 (t, J = 7.0 Hz, 2H), 2.51 (br s, 1H), 2.17 (t, J = 7.6 Hz, 2H), 1.80 (app p, J = 7.4 Hz, 2H), 1.69–1.53 (m, 4H), 1.49–1.20 (m, 48H), 1.09 (d, J = 6.8 Hz, 3H).

^{13}C NMR (101 MHz, $CDCl_3$) δ 173.4, 144.4, 144.1, 144.1, 136.7, 123.9, 98.6, 74.5, 51.6, 49.6, 44.2, 37.0, 33.7, 29.7, 29.7, 29.5, 29.5, 29.4, 29.3, 29.0, 28.6, 27.1, 26.8, 26.1, 25.9, 14.3.

HRMS calcd for $C_{40}H_{71}N_8O_5$ ($[M + H]^+$): 743.5542, found: 743.5547.

*Compound **RBM5-160**.* Compound **RBM5-142** (7 mg, 15 μmol) was added to a stirred solution of **RBM5-159** (9 mg, 12 μmol) in CH_2Cl_2 (4 mL). After stirring overnight at rt in the dark, the reaction mixture was concentrated to dryness and the residue was flash chromatographed on silica gel (from 0 to 5% MeOH in CH_2Cl_2) to afford the desired SPAAC reaction adduct **RBM5-160** (14 mg, 93%, inseparable mixture of diastereomers) as a dark-orange solid.

^{1}H NMR (400 MHz, DMSO-d_6) (mixture of diastereomers) δ 9.54 (s, 1H), 8.81 (s, 1H), 8.63 (t, J = 5.7 Hz, 1H), 8.50 (d, J = 9.1 Hz, 1H), 7.90 (d, J = 8.7 Hz, 1H), 7.49 (d, J = 8.5 Hz, 1H), 7.14–7.04 (m, 2H), 7.04 (dd, J = 8.7, 2.3 Hz, 1H), 6.41 (d, J = 9.3 Hz, 1H), 4.47 (d, J = 6.1 Hz, 1H), 4.18 (t, J = 7.0 Hz, 2H), 4.07–3.96 (m, 2H), 3.89 (s, 3H), 3.66–3.58 (m, 1H), 3.50–3.39 (m, 2H), 3.34–3.26 (m, 2H), 3.26–3.17 (m, 1H), 2.99–2.88 (m, 4H), 2.77–2.61 (m, 2H), 2.15–2.05 (m, 3H), 2.01 (t, J = 7.3 Hz, 2H), 1.73–1.60 (m, 4H), 1.56–1.05 (m, 60H), 0.97 (d, J = 6.7 Hz, 3H), 0.94–0.82 (m, 2H).

HRMS calcd for $C_{68}H_{105}N_{10}O_{11}$ ($[M + H]^+$): 1237.7959, found: 1237.7983.

*Compound **RBM5-161**.* Compound **RBM5-143** (10 mg, 15 μmol) was added to a stirred solution of **RBM5-159** (10 mg,

13 μmol) in CH_2Cl_2 (4 mL). After stirring overnight at rt in the dark, the reaction mixture was concentrated to dryness and the residue was flash chromatographed on silica gel (from 0 to 5% MeOH in CH_2Cl_2) to afford the desired SPAAC reaction adduct **RBM5-161** (16 mg, 88%, inseparable mixture of diastereomers) as a dark-red solid.

^{1}H NMR (400 MHz, DMSO-d_6) (mixture of diastereomers) δ 9.53 (br s, 1H), 8.48 (d, J = 8.9 Hz, 1H), 8.03 (d, J = 8.6 Hz, 1H), 7.94 (d, J = 2.5 Hz, 1H), 7.64–7.59 (m, 1H), 7.49 (d, J = 8.6 Hz, 1H), 7.25 (dd, J = 8.7, 2.5 Hz, 1H), 7.10 (t, J = 5.7 Hz, 1H), 6.81 (d, J = 9.2 Hz, 1H), 6.64 (d, J = 2.4 Hz, 1H), 6.38 (d, J = 9.0 Hz, 1H), 6.18 (s, 1H), 4.47 (d, J = 6.1 Hz, 1H), 4.21–4.10 (m, 4H), 4.02 (d, J = 7.8 Hz, 2H), 3.67–3.57 (m, 1H), 3.50 (q, J = 7.0 Hz, 4H), 3.46–3.39 (m, 2H), 3.25–3.18 (m, 1H), 3.15–3.04 (m, 4H), 3.05–2.95 (m, 2H), 2.94–2.86 (m, 2H), 2.78–2.59 (m, 2H), 2.13–1.90 (m, 7H), 1.83–1.73 (m, 2H), 1.70–1.59 (m, 4H), 1.54–1.10 (m, 58H), 0.96 (d, J = 6.7 Hz, 3H), 0.93–0.82 (m, 2H).

HRMS calcd for $C_{77}H_{114}N_{11}O_{10}$ ($[M + H]^+$): 1352.8745, found: 1352.8760.

Spectroscopic studies

Absorption spectra were recorded on a Jasco V-730 UV-Vis spectrophotometer using a spectral bandwidth of 1 nm, a response time of 0.24 s, a data interval of 1 nm (except for quinine sulphate and compound **RBM5-142**, in which case the data interval was of 0.2 nm) and a scan rate of 200 nm min^{-1}. Measurements were carried under an inert atmosphere (continuous flow of nitrogen gas) at a constant temperature of 20 °C.

Fluorescence emission spectra were recorded on a Photon Technology International (PTI) QuantaMaster fluorometer at room temperature. The excitation and emission monochromators were set at 0.5 mm, giving a spectral bandwidth of 2 nm (except for fluorescein and compounds **RBM5-155** and **RBM5-159**, in which case the monochromators were set at 0.35 mm, giving a spectral bandwidth of 1.4 nm). The data interval was 1 nm and the integration time was 1 s. All measurements were carried out using a Hellma 1.5 mL PTFE-stoppered fluorescence quartz cuvette (4 clear windows) with a 1 cm path length.

Molar extinction coefficients (ε) were calculated according to Lambert–Beer's law from solutions at concentrations ranging between 0.25 and 25 μM in the appropriate solvent system (spectrophotometric grade solvents). The absorbance values at the λ_{max}^{Abs} were then plotted against the corresponding concentrations and adjusted to a linear regression function forced through the origin (*i.e.* the line was forced to intercept (0,0)) using GraphPad Prism version 7.00 for Windows (GraphPad Software Inc., La Jolla, USA). Only the absorbance values in the range between 0.05 and 1 were used. Since we used a 1 cm path length cuvette, ε equals the slope of the graph.

Fluorescence quantum yields were measured (Φ_F) following the comparative method described by Resch-Genger and Rurack[41] (IUPAC technical report). The integrated fluorescence intensity (*i.e.* the area under the curve of the emission spectrum) was plotted against the corresponding Abs value at the λ_{ex} and adjusted to a linear regression function forced through the origin using GraphPad Prism version 7.00 for Windows (GraphPad Software Inc., La Jolla, CA, USA). Then, Φ_F was calculated by using eqn (1), where the subscripts x and Std. denote sample and standard, respectively, Grad equals the slope of the plot of the integrated fluorescence intensity *vs.* absorbance at the λ_{ex} and η is the refractive index of the solvent.

$$\Phi_{F,x} = \Phi_{F,Std.} \times \left(\frac{Grad_x}{Grad_{Std.}}\right) \times \left(\frac{{\eta_x}^2}{{\eta_{Std.}}^2}\right) \quad (1)$$

Spectral overlap integrals ($J(\lambda)$) of the donor–acceptor pairs were calculated using the specific $J(\lambda)$ calculator tool from a|e UV-Vis-IR Spectral Software version 2.2 for Windows from FluorTools. To calculate $J(\lambda)$, a|e UV-Vis-IR Spectral Software uses eqn (2), where F_D is the normalised donor emission spectrum, ε_A is the extinction coefficient spectrum of the acceptor, and λ is the wavelength.

$$J(\lambda) = \int_0^\infty F_D(\lambda) \times \varepsilon_A(\lambda) \times \lambda^4 d\lambda \quad (2)$$

Förster radius (R_0) of the two different donor–acceptor pairs were calculated by using eqn (3), where Φ_D is the quantum yield of the donor, $J(\lambda)$ is the spectral overlap integral, η is the refractive index of the solvent and κ is a constant that reflects the relative orientation of the excited donor's electric field and the acceptor's absorption dipole. For molecules in which the rotational diffusion of the dyes is faster than the donor's fluorescence lifetime, κ takes a value of 2/3.[42] R_0 was expressed in Å.

$$R_0 = 0.211 \times [\kappa^2 \times \Phi_D \times J(\lambda) \times \eta^{-4}]^{1/6} \quad (3)$$

Composite spectra deconvolution

The absorption and emission spectra of **RBM5-161** were decomposed into their individual components using the Composite Spectrum Regression App for OriginPro version 2018 (OriginLab Corporation, Northampton, MA, USA). The spectra of **RBM5-154** (donor) and **RBM5-143** (acceptor) were used as the reference for x_1 and x_2, respectively, to express the spectra of **RBM5-161** as the linear combination of the spectra of their individual components, according to the general eqn (4), where x_1 and x_2 are the spectra of the donor and the acceptor, respectively, multiplied for an appropriate coefficient (a_1 and a_2).

$$y = a_1x_1 + a_2x_2 \quad (4)$$

The deconvolution regression was carried out forcing an intercept with the origin, thereby obtaining a fitted curve (x_i,y_i values), the values for the a_1 and a_2 coefficients and a fitting score (R-square and SE); the reference spectra of the individual components (x_1 and x_2) were then multiplied by the a_1 and a_2 coefficients to obtain the calculated spectra.

FRET efficiency. A series of solutions of the D compounds (**RBM5-142** and **RBM5-154**) and the DA compounds (**RBM5-160** and **RBM5-161**) was prepared such that the Abs value at the

corresponding λ_{ex} was approximately between 0.01 and 0.1. The absorption and emission spectra of each solution were recorded using a 1 cm path length quartz cuvette, as described above. The absorption and emission spectra of the DA compounds were subjected to deconvolution regression using the Composite Spectrum Regression App for OriginPro version 2018 (OriginLab Corporation, Northampton, MA, USA), to isolate the spectra of the donors. The integrated fluorescence intensity was then plotted against the Abs value at the λ_{ex} and adjusted to a linear regression function forced through the origin using GraphPad Prism version 7.00 for Windows (GraphPad Software Inc., La Jolla, CA, USA). The FRET efficiency was calculated by using eqn (5), where $Grad_D$ and $Grad_{DA}$ are the slopes of the plots of the integrated fluorescence intensity *vs.* absorbance at the λ_{ex} of the donor alone and the donor component (upon spectral deconvolution) in the presence of the acceptor, respectively.

$$E = 1 - \frac{Grad_{DA}}{Grad_D} \quad (5)$$

Donor emission bleed-through (DEB). The DEB was calculated as the ratio, in the form of a percentage, between the slope of the plot of absorbance at the λ_{ex} *vs.* the integrated fluorescence intensity of the donor component upon spectral deconvolution ($Grad^{D}_{DA}$), and that of the original non-deconvoluted spectrum ($Grad^{Tot}_{DA}$) (see eqn (6)). In both cases, the fluorescence intensity was integrated for the wavelength interval corresponding to the emission of the acceptor. The data and the method used to generate the plots were the same as for the calculation of FRET efficiencies

$$DEB = \frac{Grad^{D}_{DA}}{Grad^{Tot}_{DA}} \times 100 \quad (6)$$

Acceptor emission bleed-through (AEB). This parameter was estimated following a reported protocol.[32] The AEB for the different donor–acceptor pairs were calculated as the percentage between the slopes of the plots of absorbance at the λ_{ex} *vs.* integrated fluorescence intensity corresponding to the calculated AEB spectra and to those corresponding to $F^{d}_{DA(Tot)}$ (integrated fluorescence of the non-deconvoluted spectra, being (eqn (7)).

$$AEB = \frac{Grad^{d}_{DA(AEB)}}{Grad^{d}_{DA(Tot)}} \times 100 \quad (7)$$

Cell studies

General procedures. Dulbecco's modified Eagle's medium (DMEM), fetal bovine serum (FBS), penicillin/streptomycin solution, Opti-MEM and polyethyleneimine (PEI) were from Invitrogen. Cells were cultured at 37 °C in 5% CO_2 in DMEM supplemented with 10% foetal bovine serum and 100 ng mL^{-1} each of penicillin and streptomycin.

CerS catalyzed incorporation of ωN_3PA into RBM5-155. A549 and MEF cells were seeded in 6-well plates (2×10^5 cells per well) and treated with **RBM5-155** (10 μM final concentration) and ω-azidopalmitic acid (500 μM final concentration) for 2 h. The medium was removed, the cells were washed with 400 μL PBS and harvested with 400 μL of trypsin–EDTA and 600 μL of medium. UPLC-MS analysis was performed as mentioned below. To overexpress CerS5, 24 h before transfection, HEK293T cells were seeded in 6-well plates (2×10^5 cells per well) and transfected with 2.5 μg per well of plasmid harboring the human CerS5 gene using 0.01 mg mL^{-1} of PEI in Opti-MEM for 6 h. Complete DMEM medium supplemented with 10% FBS was added and cells were incubated for 48 h. After transfection, cells were treated with **RBM5-155** and ωN_3PA as indicated above.

Lipid extraction. Cell pellets were suspended with 100 μL of H_2O and mixed with 750 μL of methanol : chloroform, 2 : 1. Samples were heated at 48 °C overnight and next day, 75 μL of 1 M KOH in methanol was added, followed by 2 h of incubation at 37 °C. Afterwards, the saponification was neutralised with 75 μL of 1 M acetic acid and solvent was removed using a Speed Vac Savant SPD131DDA (Thermo Scientific).

UPLC-MS analysis. Lipid extracts, fortified with internal standards (*N*-dodecanoylsphingosine, *N*-dodecanoylglucosylsphingosine, *N*-dodecanoylsphingosylphosphorylcoline and C17-sphinganine, 0.2 nmol each) were solubilised in 150 μL of methanol. Samples were then centrifuged at 9300*g* for 3 min and 130 μL of the supernatant was injected into a Waters Aquity UPLC system connected to a Waters LCT Premier Orthogonal Accelerated Time of Flight Mass Spectrometer (Waters, Milford, MA, USA) operated in the positive electrospray ionisation mode. Full scan spectra from 50 to 1500 Da were acquired and individual spectra were summed to produce data points every 0.2 s. Mass accuracy and reproducibility were maintained by using an independent reference from LockSpray. The analytical column was a 100 mm × 2.1 mm i.d., 1.7 μm C8 Acquity UPLC BEH (Waters). The two mobile phases were phase A: methanol/water/formic acid (74/25/1 v/v/v) and phase B: methanol/formic acid (99/1 v/v), and both also contained 5 mM ammonium formate. A linear gradient was programmed—0.0 min: 80% B; 3 min: 90% B; 6 min: 90% B; 15 min: 99% B; 18 min: 99% B; 20 min: 80% B. The flow rate was 0.3 mL min^{-1}.

Conflicts of interest

There are no conflicts to declare.

Acknowledgements

Partial financial support from the Project CTQ2017-85378-R (AEI/FEDER, UE) of the Spanish Ministry of Science, Innovation and Universities is acknowledged. We are grateful to Prof. Anthony H. Futerman (Weizmann Institute of Science, Rehovot, Israel) for providing the CerS5 plasmid and to Prof. Vicente Marchán (UB) for technical support. Experimental contributions from Mr Alexandre García and Mr Pedro Rayo are

also acknowledged. About the source of the cells, we purchased from ATCC (https://www.lgcstandards-atcc.org/en.aspx). We acknowledge support of the publication fee by the CSIC Open Access Publication Support Initiative through its Unit of Information Resources for Research (URICI).

References

1 A. C. Carreira, T. C. Santos, M. A. Lone, E. Zupančič, E. Lloyd-Evans, R. F. M. de Almeida, T. Hornemann and L. C. Silva, Mammalian Sphingoid Bases: Biophysical, Physiological and Pathological Properties, *Prog. Lipid Res.*, 2019, **75**, 100988.

2 Y. A. Hannun and L. M. Obeid, Principles of Bioactive Lipid Signalling: Lessons from Sphingolipids, *Nat. Rev. Mol. Cell Biol.*, 2008, **9**(2), 139–150.

3 A. Alonso and F. M. Goñi, The Physical Properties of Ceramides in Membranes, *Annu. Rev. Biophys.*, 2018, **47**(1), 633–654.

4 Y. A. Hannun, Functions of Ceramide in Coordinating Cellular Responses to Stress, *Science*, 1996, **274**(5294), 1855–1859.

5 G. M. Jenkins, A. Richards, T. Wahl, C. Maos, L. Obeid and Y. A. Hannun, Involvement of Yeast Sphingolipids in the Heat Stress Response of Saccharomyces Cerevisiae, *J. Biol. Chem.*, 1997, **272**, 32566–32572.

6 H. Sietsma, R. J. Veldman and J. W. Kok, The Involvement of Sphingolipids in Multidrug Resistance, *J. Membr. Biol.*, 2001, **181**, 153–162.

7 S. M. Cho and H. J. Kwon, Acid Ceramidase, an Emerging Target for Anti-Cancer and Anti-Angiogenesis, *Arch. Pharmacal Res.*, 2019, **42**(3), 232–243.

8 T. Okazaki, R. M. Bell and Y. A. Hannun, Sphingomyelin Turnover Induced by Vitamin D3 in HL-60 Cells. Role in Cell Differentiation, *J. Biol. Chem.*, 1989, **264**(32), 19076–19080.

9 M. E. Venable, J. Y. Lee, M. J. Smyth, A. Bielawska and L. M. Obeid, Role of Ceramide in Cellular Senescence, *J. Biol. Chem.*, 1995, **270**(51), 30701–30708.

10 T. D. Mullen, Y. A. Hannun and L. M. Obeid, Ceramide Synthases at the Centre of Sphingolipid Metabolism and Biology, *Biochem. J.*, 2012, **441**, 789–802.

11 J. Kurz, M. J. Parnham, G. Geisslinger and S. Schiffmann, Ceramides as Novel Disease Biomarkers, *Trends Mol. Med.*, 2018, **25**(1), 20–32.

12 J. Stiban, R. Tidhar and A. H. Futerman, Ceramide Synthases: Roles in Cell Physiology and Signaling, *Adv. Exp. Med. Biol.*, 2010, **688**, 60–71.

13 J. W. Park, W. J. Park and A. H. Futerman, Ceramide Synthases as Potential Targets for Therapeutic Intervention in Human Diseases, *Biochim. Biophys. Acta, Mol. Cell Biol. Lipids*, 2014, **1841**(5), 671–681.

14 A. H. Merrill Jr., M. C. Sullards, J. C. Allegood, S. Kelly and E. Wang, Sphingolipidomics: High-Throughput, Structure-Specific, and Quantitative Analysis of Sphingolipids by Liquid Chromatography Tandem Mass Spectrometry, *Methods*, 2005, **36**(2), 207–224.

15 S. Grösch, S. Schiffmann and G. Geisslinger, Chain Length-Specific Properties of Ceramides, *Prog. Lipid Res.*, 2012, **51**(1), 50–62.

16 I. Nieves, P. Sanllehí, J.-L. L. Abad, G. Fabriàs, J. Casas and A. Delgado, Chemical Probes of Sphingolipid Metabolizing Enzymes, in *Bioactive Sphingolipids in Cancer Biology and Therapy*, ed. Y. Hannun, C. Luberto, L. Obeid and C. Mao, Springer International Publishing, Cham, 2015, pp. 437–469.

17 J. L. Abad, I. Nieves, P. Rayo, J. Casas, G. Fabriàs and A. Delgado, Straightforward Access to Spisulosine and 4,5-Dehydrospisulosine Stereoisomers: Probes for Profiling Ceramide Synthase Activities in Intact Cells, *J. Org. Chem.*, 2013, **78**(12), 5858–5866.

18 An initial version of this work was deposited in ChemRxiv on August 6, 2020, DOI: 10.26434/chemrxiv.127641.

19 S. Haldar and A. Chattopadhyay, in *Application of NBD-Labeled Lipids in Membrane and Cell Biology*, ed. Y. Mély and G. Duportail, Springer Berlin Heidelberg, 2012, pp. 37–50.

20 P. J. G. Coutinho, Photophysics and Biophysical Applications of Benzo[a]Phenoxazine Type Fluorophores, in *Reviews in Fluorescence*, Springer, New York, NY, 2009, vol. 2007, pp. 335–362.

21 O. Wichmann, M. H. Gelb and C. Schultz, Probing Phospholipase A2 with Fluorescent Phospholipid Substrates, *ChemBioChem*, 2007, **8**(13), 1555–1569.

22 O. Wichmann, J. Wittbrodt and C. Schultz, A Small-Molecule FRET Probe To Monitor Phospholipase A2 Activity in Cells and Organisms, *Angew. Chem., Int. Ed.*, 2006, **45**(3), 508–512.

23 O. Wichmann and C. Schultz, FRET Probes to Monitor Phospholipase A2 Activity, *Chem. Commun.*, 2001, **1**(23), 2500–2501.

24 K. P. Bhabak, A. Hauser, S. Redmer, S. Banhart, D. Heuer and C. Arenz, Development of a Novel FRET Probe for the Real-Time Determination of Ceramidase Activity, *ChemBioChem*, 2013, **14**(9), 1049–1052.

25 T. Pinkert, D. Furkert, T. Korte, A. Herrmann and C. Arenz, Amplification of a FRET Probe by Lipid–Water Partition for the Detection of Acid Sphingomyelinase in Live Cells, *Angew. Chem., Int. Ed.*, 2017, **56**(10), 2790–2794.

26 J. G. Mina, J. A. Mosely, H. Z. Ali, P. W. Denny and P. G. Steel, Exploring Leishmania Major Inositol Phosphorylceramide Synthase (LmjIPCS): Insights into the Ceramide Binding Domain, *Org. Biomol. Chem.*, 2011, **9**(6), 1823–1830.

27 P. K. Mandal and J. S. McMurray, Pd–C-Induced Catalytic Transfer Hydrogenation with Triethylsilane, *J. Org. Chem.*, 2007, **72**(17), 6599–6601.

28 In this sense, our early attempts to obtain the free amine by washing the organic extracts with 0.5 M NaOH resulted in the formation of unidentified by-products, as evidenced by the appearance of new UV active spots in the TLC plate, and a poor recovery after column chromatography of the crude.

29 T. Walter, J. Schlegel, A. Burgert, A. Kurz, J. Seibel and M. Sauer, Incorporation Studies of Clickable Ceramides in Jurkat Cell Plasma Membranes, *Chem. Commun.*, 2017, **53**(51), 6836–6839.

30 J. Dommerholt, S. Schmidt, R. Temming, L. J. A. Hendriks, F. P. J. T. Rutjes, J. C. M. van Hest, D. J. Lefeber, P. Friedl and F. L. van Delft, Readily Accessible Bicyclononynes for Bioorthogonal Labeling and Three-Dimensional Imaging of Living Cells, *Angew. Chem., Int. Ed.*, 2010, **49**(49), 9422–9425.

31 I. Tosi, *Model Systems for Artificial Photosynthesis: Calix[4] Arenes Functionalized with Chromophoric Units for Energy and Charge Transfer*, Doctoral thesis, Universita' degli studi di Parma, 2015.

32 E. A. Bykova and J. Zheng, Spectra FRET: A Fluorescence Resonance Energy Transfer Method in Live Cells, in *Reviews in Fluorescence 2007*, ed. C. D. Geddes, Springer, New York, NY, 2009, pp. 87–101.

33 S. Smith, A. Witkowski and A. K. Joshi, Structural and Functional Organization of the Animal Fatty Acid Synthase, *Prog. Lipid Res.*, 2003, **42**(4), 289–317.

34 S. A. McCune and R. A. Harris, Mechanism Responsible for 5-(Tetradecyloxy)-2-Furoic Acid Inhibition of Hepatic Lipogenesis, *J. Biol. Chem.*, 1979, **254**(20), 10095–10101.

35 D. L. Halvorson and S. A. McCune, Inhibition of Fatty Acid Synthesis in Isolated Adipocytes by 5-(Tetradecyloxy)-2-Furoic Acid, *Lipids*, 1984, **19**(11), 851–856.

36 D. Vance, I. Goldberg, O. Mitsuhashi, K. Bloch, S. Ōmura and S. Nomura, Inhibition of Fatty Acid Synthetases by the Antibiotic Cerulenin, *Biochem. Biophys. Res. Commun.*, 1972, **48**(3), 649–656.

37 S. Lahiri, H. Lee, J. Mesicek, Z. Fuks, A. Haimovitz-Friedman, R. N. Kolesnick and A. H. Futerman, Kinetic Characterization of Mammalian Ceramide Synthases: Determination of Km Values towards Sphinganine, *FEBS Lett.*, 2007, **581**(27), 5289–5294.

38 S. Lahiri and A. H. Futerman, LASS5 Is a Bona Fide Dihydroceramide Synthase That Selectively Utilizes Palmitoyl-CoA as Acyl Donor, *J. Biol. Chem.*, 2005, **280**(40), 33735–33738.

39 A. N. Rai and A. Basu, Sphingolipid Synthesis via Olefin Cross Metathesis: Preparation of a Differentially Protected Building Block and Application to the Synthesis of D-Erythro-Ceramide, *Org. Lett.*, 2004, **6**(17), 2861–2863.

40 T. Ibuka, H. Habashita, A. Otaka, N. Fujii, Y. Oguchi, T. Uyehara and Y. Yamamoto, A Highly Stereoselective Synthesis of (E)-Alkene Dipeptide Isosteres via Organocyanocopper-Lewis Acid Mediation Reaction, *J. Org. Chem.*, 1991, **56**(14), 4370–4382.

41 U. Resch-Genger and K. Rurack, Determination of the Photoluminescence Quantum Yield of Dilute Dye Solutions (IUPAC Technical Report), *Pure Appl. Chem.*, 2013, **85**(10), 2005–2013.

42 S. M. Müller, H. Galliardt, J. Schneider, B. George Barisas and T. Seidel, Quantification of Förster Resonance Energy Transfer by Monitoring Sensitized Emission in Living Plant Cells, *Front. Plant Sci.*, 2013, 413, Frontiers Research Foundation.